Comparative study on transport properties of N-, P-, and As-doped SiC nanowires: Calculated based on first principles*

Ya-Lin Li(李亚林), Pei Gong(龚裴), and Xiao-Yong Fang(房晓勇)†

Key Laboratory for Microstructural Material Physics of Hebei Province, School of Science, Yanshan University, Qinhuangdao 066004, *China*

(Received 15 December 2019; revised manuscript received 13 January 2020; accepted manuscript online 16 January 2020)

According to the one-dimensional quantum state distribution, carrier scattering, and fixed range hopping model, the structural stability and electron transport properties of N-, P-, and As-doped SiC nanowires (N-SiCNWs, P-SiCNWs, and As-SiCNWs) are simulated by using the first principles calculations. The results show that the lattice structure of N-SiCNWs is the most stable in the lattice structures of the above three kinds of doped SiCNWs. At room temperature, for unpassivated SiCNWs, the doping effect of P and As are better than that of N. After passivation, the conductivities of all doped SiCNWs increase by approximately two orders of magnitude. The N-SiCNW has the lowest conductivity. In addition, the N-, P-, As-doped SiCNWs before and after passivation have the same conductivity–temperature characteristics, that is, above room temperature, the conductivity values of the doped SiCNWs all increase with temperature increasing. These results contribute to the electronic application of nanodevices.

Keywords: N-, P-, As-doped SiC nanowires, transport properties, first-principles theory

PACS: 73.63.–b, 61.72.U–, 63.20.dk, 81.07.Gf **DOI:** 10.1088/1674-1056/ab6c4c

1. Introduction

Silicon carbide (SiC) is an extremely attractive material because of its mechanical property, thermal stability, heat transfer performance, and chemical stability.[1,2] SiC nanostructures, such as nanocrystals, nanowires, nanoribbons, and nanotubes, have wide band gap, high atomic binding energy, high electron saturation mobility, high critical excitation field strength, high thermal conductivity, and strong radiation resistance,[3–8] and are widely used in high frequency, high power, high temperature, radiation resistant electronic and optoelectronic devices.[9–12] As an important component of silicon carbide nanomaterials, SiC nanowires (SiCNWs) have recived the attention.[13–17] A lot of researches show that SiCNWs have potential applications in hydrogen storage field,[18] photoelectron device,[19–22] electromagnetic shielding and absorption.[23–26]

Doping is one of the best ways to obtain excellent properties of SiCNWs.[27,28] In recent years, many researchers have studied the substitutional doping of SiCNWs. Of them, the elements of the third and fifth main groups are the most common dopants. For instance, Yang *et al.* reported the growth of p-type 3C-SiCNWs with B dopants and sharp corners produced via the catalyst-assisted pyrolysis of a polymeric precursor, and the research indicated that the high-temperature field emission (FE) stability of SiCNWs could be significantly enhanced by the B dopants.[29] Zhao *et al.* obtained the nitrogen-doped SiCNWs by chemical vapor reaction method, and studied their FE performance from two aspects of calculation and testing, and the results showed that when the N content takes an optimal value the N-doped SiCNWs can act as a candidate for field emitters with very low turn-on fields and threshold fields.[30] In 2015, Chen *et al.* found that the supercapacitor performance of SiCNW arrays can be substantially enhanced by nitrogen doping, which could favor a more localized impurity state near the conduction band edge which greatly improves the quantum capacitance and hence increases the bulk capacitance and the high-power capability[31] In 2017, Li *et al.* studied the effects of different vacancies on the electrical and optical properties of SiCNWs.[16] In 2018, Li *et al.* investigated the electrical and optical properties of SiCNWs and doped SiCNWs of different diameters,[13] and the results show that surface dangling bonds can inhibit the quantum size effect in SiCNWs,[2] and thus leading the impurity band to be discretized.[32] In fact, the studies on the effects of doping on performance have focused on electrical properties, optical properties, and magnetic properties.[8,22,27,33–35] It can be seen from the above literature that the donor is mostly concentrated in the nitrogen (N) atom, while the acceptor is concentrated in the boron (B) atom. So far, the systematic research on the transport characteristics of the fifth group-doped SiCNWs has not been reported. As is well known, the semiconductor conductivity is closely related to the transport process of carriers. Therefore, it is important for the development of nanoelectronic devices to study the electron transport properties of doped SiCNWs.

In this paper, we systematically study the structural stabil-

*Project supported by the National Natural Science Foundation of China (Grant No. 11574261) and the Natural Science Foundation of Hebei Province, China (Grant No. A2015203261).

†Corresponding author. E-mail: fang@ysu.edu.cn

ity of N-, P-, and As-SiCNWs, numerically simulate the transport properties of N-, P-, and As-doped SiCNWs, and compared their doping effects. The results provide an important basis for selecting the optimum donor impurities of SiCNWs.

2. Computational methods and models

2.1. Doped SiCNWs model

In this paper, the outer three layers were cut into a vacuum layer on the $(6\times6\times1)$ SiCNWs structure, and the $(3\times3\times1)$ hexagonal cross-section SiCNWs were established. We used the CASTEP software based on density functional theory (DFT) in Material Studio 6.0 to optimize all structures, and the generalized gradient approximation (GGA) and ultra-soft pseudopotential (PBE) were also used. In the optimization settings, the cut-off energy of the plane wave was set to be 340 eV, the point k of the Monkhorst–Pack grid was set to be $1\times1\times8$ in the first Brillouin zone, and the energy individual-atom, the interaction between atoms , the maximum shift of atoms , and the internal stress of the crystal are assumed to converge to 2.0×10^{-5} eV, 0.05 eV/Å, 0.002 Å, and 0.1 GPa, respectively. In order to establish the doping model for each of N-, P-, As-SiCNWs (as shown in Fig. 1), the fifth group elements N, P, As substituted for the same carbon atom (C) in SiCNWs, respectively. For the undoped and doped model, the structural optimization and properties' simulation were performed, and thus providing basic data for conductivity calculations.

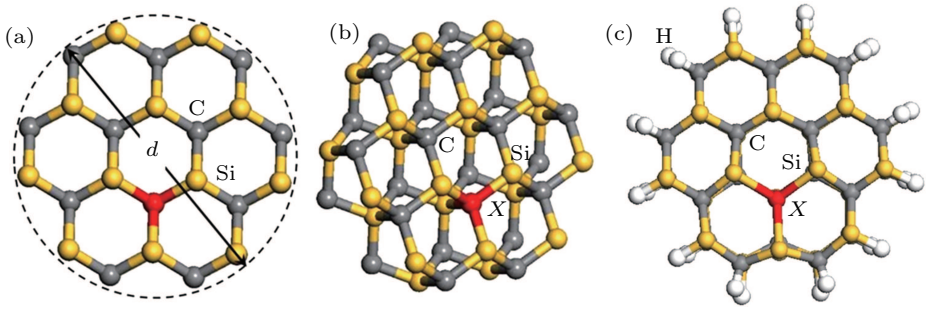

Fig. 1. Lattice structure of doped SiCNWs showing (a) cross section, (b) side of doped SiCNW, and (c) cross section of hydrogen passivation-doped SiCNWs, with d being the diameter of cross section of nanowire and X representing N, P, and As separately.

2.2. Conductivity of doped SiCNWs

In the energy range ε–$(\varepsilon+\mathrm{d}\varepsilon)$, electronic state of the nanowire can be written as follows:

$$D(\varepsilon)\,\mathrm{d}\varepsilon=\frac{2L}{h}\left(\frac{m^*}{2}\right)^{1/2}\varepsilon^{-1/2}\mathrm{d}\varepsilon, \tag{1}$$

where L represents the length of the nanowires, m^* the effective mass of the carrier, and h the Planck's constant. Considering that the carrier concentration in semiconductor is much lower than that of free electron concentration in metal, the carrier distribution can be described by the Boltzmann function.[36] For an n-type SiCNW with length L and cross-sectional area S, the electron concentration is expressed as

$$\begin{aligned} n &= \frac{2}{Sh}\left(\frac{m^*}{2}\right)^{1/2}\int_{\varepsilon_\mathrm{d}}^{\infty}\varepsilon^{1/2}\exp\left(-\frac{\varepsilon-\varepsilon_\mathrm{F}}{k_\mathrm{B}T}\right)\mathrm{d}\varepsilon \\ &= \frac{\sqrt{2m^*\pi k_\mathrm{B}T}}{Sh}\exp\left(-\frac{\varepsilon_\mathrm{d}-\varepsilon_\mathrm{F}}{k_\mathrm{B}T}\right), \end{aligned} \tag{2}$$

where ε_d and ε_F represent the energy of the bottom of the impurity band and the Fermi level, respectively.

As can be seen from Ref. [32], the dangling bonds on the surface of the doped SiCNWs cause the impurity bands to be discretized. When electrons are transported within the discretized impurity band, its mobility can be expressed as

$$\mu_1=\frac{ev_\mathrm{ph}R^2}{6k_\mathrm{B}T}\exp\left(-2\alpha R-\frac{W}{k_\mathrm{B}T}\right), \tag{3}$$

where v_ph denotes the atomic vibration frequency (phonon frequency) and R the electron transition distance (impurity spacing). The hopping activation energy W is determined by the electron density of states $D(\varepsilon_\mathrm{F})$ at the Fermi level, that is, $W=1/D(\varepsilon_\mathrm{F})$. The spatial extensibility of wave function $1/\alpha$ can be estimated according to the uncertainty relation $\Delta x\cdot\Delta p\geq h/2\pi$, that is, $\alpha\leq2\pi\delta/c$, where c is the lattice constant of SiCNW and δ is the k-point accuracy determined by grid parameters.[35]

After passivation, the discrete impurity band forms a degenerate impurity level. In this case, electron mobility is mainly determined by optical phonon scattering, ionized impurity scattering and neutral impurity scattering, and can be expressed as[36]

$$\mu_2=\frac{e}{m^*}\left(\frac{1}{\tau_\mathrm{opt}}+\frac{1}{\tau_\mathrm{ion}}+\frac{1}{\tau_\mathrm{neu}}\right)^{-1}, \tag{4}$$

$$\frac{1}{\tau_\mathrm{opt}}=\frac{\mathrm{e}^2\left(2m^*\hbar\omega_\mathrm{opt}\right)^{1/2}}{4\pi\varepsilon_0\hbar^2\left(\mathrm{e}^{\hbar\omega_\mathrm{opt}/k_\mathrm{B}T}-1\right)}\left(\frac{1}{\varepsilon_\mathrm{opt}}-\frac{1}{\varepsilon_\mathrm{s}}\right), \tag{5}$$

$$\frac{1}{\tau_\mathrm{ion}}=\frac{N_\mathrm{ion}\mathrm{e}^4}{8\pi\left(m^*\varepsilon_0\varepsilon_\mathrm{s}\right)^2\bar{v}^3}\ln\left[1+\left(\frac{2\pi m^*\varepsilon_0\varepsilon_\mathrm{s}\bar{v}^2}{N_\mathrm{ion}^{1/3}\mathrm{e}^2}\right)^2\right], \tag{6}$$

$$\frac{1}{\tau_\mathrm{neu}}=20\hbar N_\mathrm{neu}\frac{4\pi\varepsilon_0\varepsilon_\mathrm{s}\hbar^2}{\mathrm{e}^2m^{*2}}, \tag{7}$$

where ω_opt is the optical phonon frequency, ε_s and ε_opt are the static and high frequency-relative dielectric constant, respec-

tively, N_{ion} and N_{neu} are the concentration of ionized impurities and non-ionized impurities, respectively. For one-dimensional SiCNW, the average thermal motion velocity of electrons is

$$\bar{v} = \sqrt{\frac{9\pi k_B T}{8m^*}}. \tag{8}$$

3. Results and discussion

3.1. First-principles calculation

3.1.1. Structural stability

By calculating the binding energy, the lattice structure stability of doped SiCNW can be compared. For the N-, P-, and As-doped SiCNWs, the binding energy can be obtained from the following equation:

$$E_B = \frac{E_T - E_{Si}N_{Si} - E_C N_C - E_d N_d}{N}, \tag{9}$$

where E_T is the total energy of N-, P-, As-SiCNWs, and E_{Si}, E_C, and E_d are the free energy of Si, C, and doped atoms, and N_{Si}, N_C, and N_d are the numbers of atoms of Si, C, and doped atom, respectively. Total number of atoms N is 48. Detailed data are shown in Table 1.

Table 1. Lattice structure parameters of SiCNW and N-, P-, As-SiCNWs.

Structures	Lattice constant/Å		Atomic number			Atomic free energy/eV			Total energy E_T/eV	Binding energy
	a	c	N_{Si}	N_C	N_d	E_{Si}	E_C	E_d		E_B/(eV/atom)
SiCNWs	3.078	5.114	24	24	0	–101.52	–145.84	–	–6282.94	–7.215
N-SiCNWs	3.085	5.093	24	23	1	–101.52	–145.84	–261.71	–6399.19	–7.223
P-SiCNWs	3.117	5.152	24	23	1	–101.52	–145.84	–174.33	–6306.40	–7.11
As-SiCNWs	3.125	5.163	24	23	1	–101.52	–145.84	–167.48	–6297.97	–7.077

As can be seen from Table 1, compared with the binding energy of SiCNWs, the binding energy of N-, P-, and As-doped SiCNWs changes by 0.10%, 1.45%, and 1.9%, respectively, which indicates that the fifth group doping has little effect on the structural stability of SiCNWs. Of the four atoms of C, N, P, and As, the N atom has the largest electronegativity and the smallest atomic radius; when N replaces the C atom, the N–Si bond is stronger than the C–Si bond, so the structure of the N–SiCNWs is more stable than the undoped SiCNWs. For P and As atoms, their electronegativities are less than the electronegativity of C atom, and their atomic radii are larger than the radius of C atom, therefore, the doping of P and As leads the stability of SiCNWs to decrease slightly.

3.1.2. Electron energy bands and state density

Figures 2 and 3 show the band structure and electronic density distribution of the undoped and doped SiCNWs, the associated data are shown in Table 2.

It can be seen from Fig. 2 that the conduction band of undoped SiCNWs consists of two parts that are almost connected, and the lower part comes from the surface dangling bonds,[37] which will introduce an impurity band and lead the band gap to decrease. However, since the number of cleavage bonds of the surface Si atom and that of surface C atom are the same, there is no free electron in the impurity band.

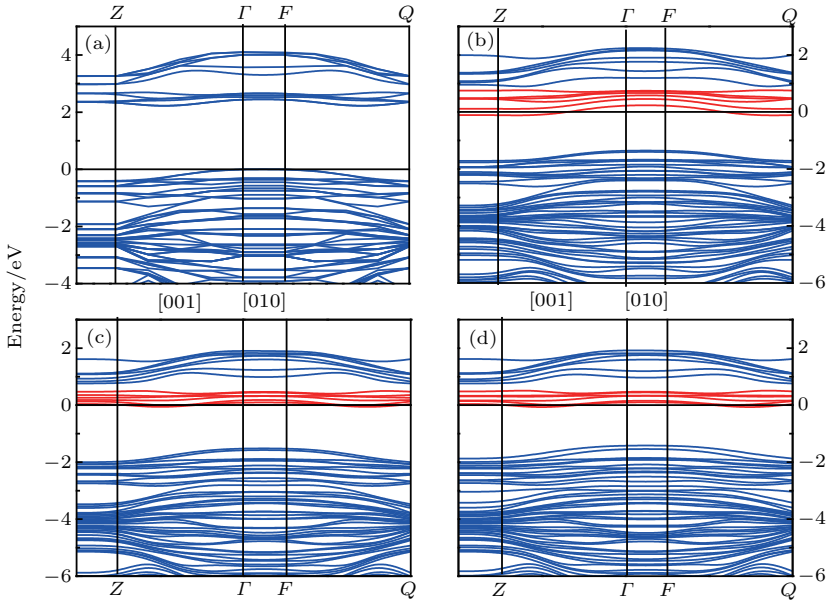

Fig. 2. Band structures of (a) undoped SiCNWs, (b) N-SiCNWs, (c) P-SiCNWs, and (d) As-SiCNWs.

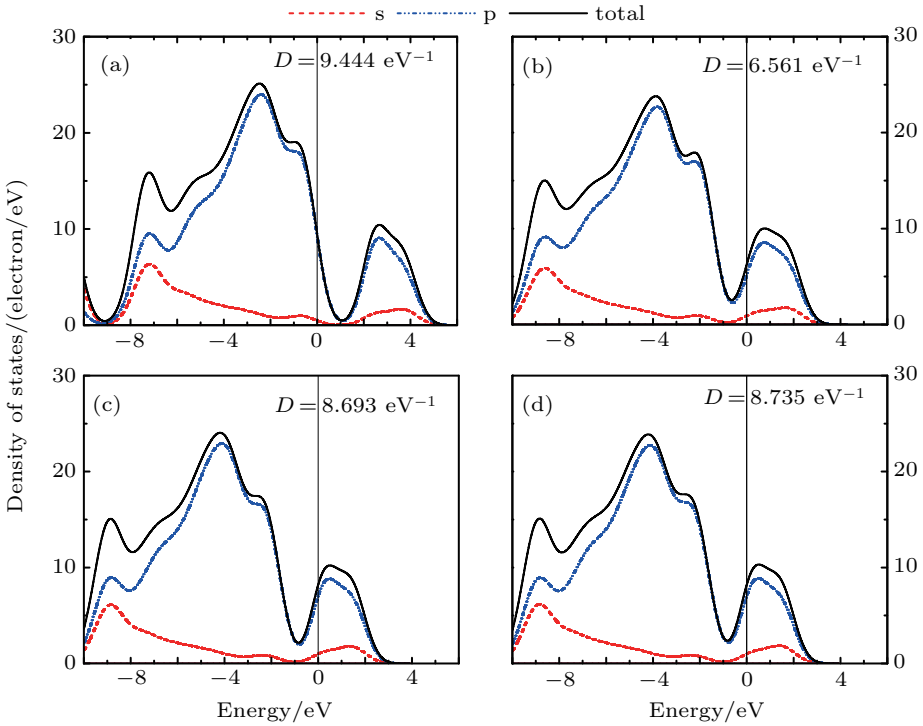

Fig. 3. Distribution of density of states for (a) undoped SiCNWs, (b) N-SiCNWs, (c) P-SiCNWs, (d) As-SiCNWs, where green line denotes the total state density, blue line the p-state electron, and red line the s-state electron.

Table 2. Numerical simulation parameters of SiCNWs and N-, P-, As-SiCNWs. According to the setting of the k-point grid parameter, δ is taken to be 0.08.[35] Dielectric constant $\varepsilon_s = 10.3$, and high frequency dielectric constant $\varepsilon_{opt} = 1.7$.[35] The other parameters are derived from first principles calculations.

Structures	Spatial extensibility $(1/\alpha)$/nm*	Electron jump distance R/nm	Effective mass m^*/m_e	Acoustic phonon frequency v_{ph}/THz	Optical phonon frequency v_{ph}/THz	Impurity band bottom ε_d/eV	State density $D(\varepsilon_F)$/(1/eV)
SiCNWs	1.0179	0.5114	1.48/1.82	6.87	17	2.218	9.444
N-SiCNWs	1.0138	0.5093	1.45	6.87	17	–0.1279	6.561
P-SiCNWs	1.0255	0.5152	1.70	6.87	17	–0.0713	8.693
As-SiCNWs	1.0277	0.5163	1.51	6.87	17	–0.0834	8.735

For doped SiCNW, substitution of N, P, and As for C atoms produces weakly bonded electrons, and thus causing common electrons to appear on the impurity band to form an n-type semiconductor. After being doped , SiCNWs become an indirect bandgap semiconductor, in which the valence band tops of all SiCNWs are in the center Γ of the Brillouin zone, the bottom of the conduction band (the bottom of the impurity) appears in the [001] direction and is at a quarter of the boundary of the Brillouin zone. It may follow from the distribution of electronic density of states (Fig. 3) that in SiCNWs, p electrons play a leading role, the valence band top is determined by the 2p electron of C atom, and the 3p electron of Si atom mainly affects the conduction band.[2,13] This indicates that the density of states $D(\varepsilon_F)$ near the Fermi level of undoped SiCNWs is determined by the 2p electronic state of C atom. The value density $D(\varepsilon_F)$ near the Fermi level of the doped SiCNWs is mainly determined by the 3p electrons of Si atom, which are affected by p-state electrons of doping atom such as N, P, and As atoms.[32]

3.2. Transport properties for N-, P-, As-SiCNTs based on numerical simulations

3.2.1. Doping effect of different acceptor

According to Eqs. (1)–(8) and Tables 1 and 2, we calculate the doping effect of the fifth group elements N, P, and As on SiCNWs before and after H passivation. The numerical simulation results of electron concentration and mobility and conductivity at room temperature ($T = 300$ K) are shown in Fig. 4. It can be seen that the mobility of undoped SiCNWs is greater than that of doped SiCNWs. However, due to the low carrier concentration of undoped SiCNWs, its conductivity (8.0×10^{-20} S/cm) is much lower than the conductivity of doped SiCNWs (not shown in Fig. 4).

It can be seen from Fig. 4(a) that the conductivity ($T = 300$ K) of N-SiCNWs is less than one-quarter of P- and As-SiCNWs, while the difference in quantity between P and As dopings is small. The difference in carrier concentration produced among N, P, and As dopings is small, and their doping effect is mainly derived by mobility. From Fig. 2, the surface dangling bond of N-SiCNWs has a large discrete ef-

fect on the impurity band, which makes the value of $D(\varepsilon_F)$ smaller (Fig. 3), therefore, the electron mobility in N-SiCNWs is smaller than that of P- and As-SiCNWs. After the surface dangling bonds are saturated with hydrogen, the conductivity of N-, P-, and As-SiCNWs are increased by about two orders of magnitude (at room temperature) as shown in Fig. 4(b). This is because the interaction between the surface state of the dangling bond and the impurity level disappears, and thus causing the discretized impurity band to form a degenerate impurity level, at this time, the electron migration follows the Boltzmann transport theory rather than the VRH model. The main factor affecting migration is the scattering mechanism. Figure 4(b) shows that after passivation, the conductivity of N-SiCNWs is still smallest, but the difference is not large (less than 20%).

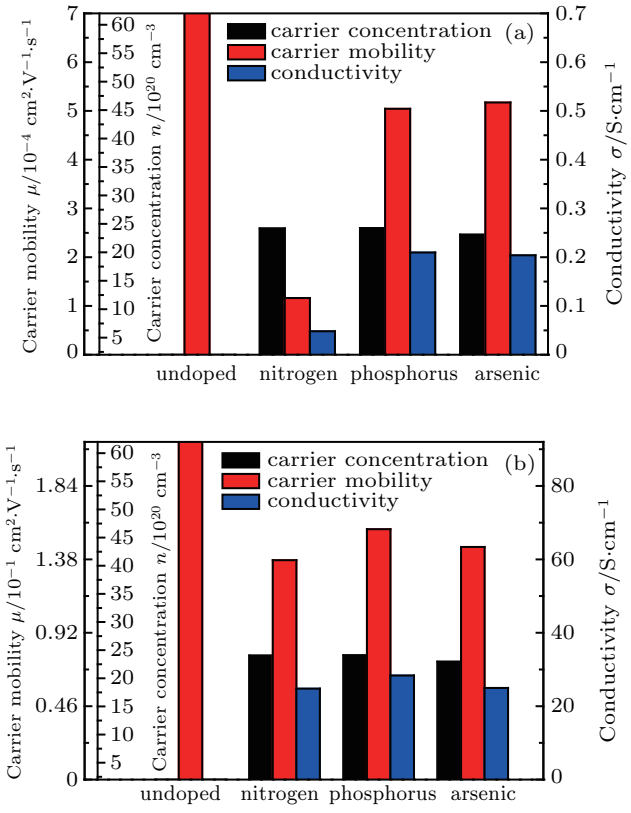

Fig. 4. Schematic diagram of different donor doping effects for (a) unpassivated N-, P-, As-SiCNWs and (b) passivated N-, P-, As-SiCNWs.

3.2.2. Temperature-dependent conductivity and thermal stability of conductivity

Based on first-principles data in Tables 1 and 2, using the carrier concentration and mobility Eqs. (1)–(8) of the resonances, the temperature characteristics of the conductivity of the N-, P-, As-SiCNWs (unpassivated and passivated) and the temperature coefficient of the conductivity (TCC)[38] at different temperatures are obtained as shown in Fig. 5. The temperature characteristics of carrier mobility of the N-, P-, As-SiCNWs (unpassivated and passivated) are shown in Fig. 6.

It can be seen from Fig. 5(a) that the conductivity of the N-, P-, As-SiCNWs increase with temperature increasing, while at temperatures below 300 K, the conductivity does not change much with temperature increasing. At all temperatures above 300 K, the conductivity of P-SiCNWs and As-SiCNWs are more considerable than that of N-SiCNWs, and the conductivity of P-SiCNWs is slightly greater than that of As-SiCNWs. After passivation, the temperature characteristics of the conductivity of N-, P-, and As-SiCNWs are similar to those of unpassivated SiCNWs. At all temperatures, the conductivity of P-SiCNWs is more considerable than that of N- and As-SiCNWs as shown in Fig. 5(b). Regarding the effect of diameter effect on conductivity, according to the previous work,[13,30] we can speculate that as the size increases, the doping concentration will decrease and so will the conductivity.

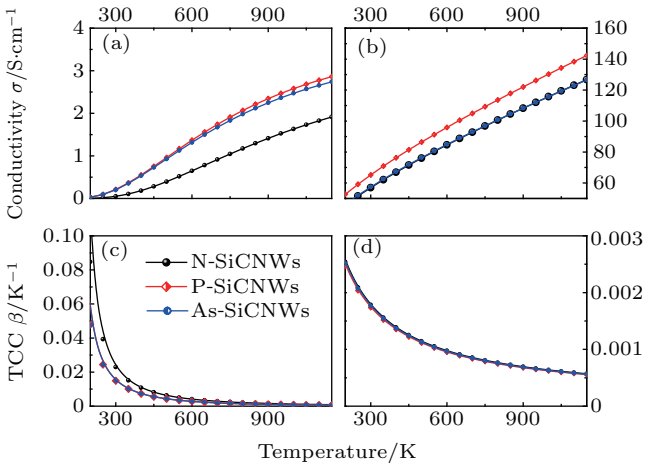

Fig. 5. Plots of temperature-dependent conductivity and temperature coefficient of [(a) and (c)] unpassivated and [(b) and (d)] passivated N-, P-, As-SiCNWs.

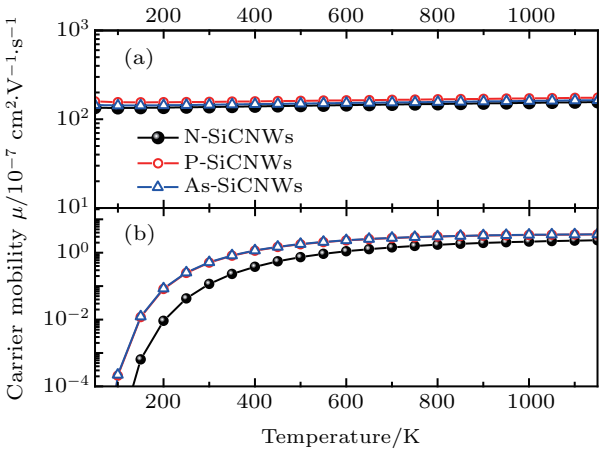

Fig. 6. Temperature-dependent carrier mobility of (a) passivated and (b) unpassivated N-, P-, As-SiCNWs.

It can be seen from Figs. 5(c) and 5(d) that the TCC values decrease with temperature increasing. Among them, the TCC value of N-, P-, and As-SiCNWs at room temperature are all about 2% K^{-1}, the three dopants are slightly different

from each other. After passivation, there is almost no difference in TCC value among the three dopants, their TCC values are increase by an order of magnitude (about 0.2% K^{-1}). This indicates that the passivation improves the thermal stability of N-, P-, and As-SiCNWs.

The mobilities of the bare N-, P-, As-SiCNWs increase with temperature increasing and tend to a constant value (about 3.5×10^{-3} $cm^2/V{\cdot}s$). The dependences of the carrier mobility of passivated N-, P-, As-SiCNWs on temperature are very small. Due to the small difference in the carrier concentration among the doped SiCNWs, the high conductivity of P-SiCNWs is mainly because of their high mobility. As can be seen from Figs. 2, 5, and 6, among doped SiCNWs, below 300 K, the mobility plays a dominant role in the conductivity, while above 300 K, the leading role is the carrier concentration.

4. Conclusions

In summary, we have used the generalized gradient approximation method in density functional theory to study the conductance spectra of the fifth group of N-, P-, As-doped SiCNWs. Based on the data of the band structure, we calculate the transmission characteristics of the doped SiCNWs. The results show that N-doping is the most stable in all doped SiCNWs. At room temperature, for unpassivated SiCNWs, the doping effects of P and As are better than that of N. After passivation of SiCNWs, the conductivity values of all doped SiCNWs increase by approximately two orders of magnitude. The conductivity of N-SiCNWs is still smallest, but it is not much different from others. The conductivity of the N-, P-, As-SiCNWs before and after passivation are compared, showing that the three doped SiCNWs have the same conductivity-temperature characteristics, that is, above room temperature, the conductivity of the doped SiCNWs increases with temperature increasing. Of them, P-doped SiCNWs have the highest conductivity. The TCCs of N-, P-, As-doped SiCNWs (before and after passivation) all decrease with temperature increasing, and the passivation can improve the thermal stability for each cof N-, P-, and As-doped SiCNWs.

References

[1] Fan Y, Wu X L, Zhao P Q and Chu P K 2006 *Phys. Lett. A* **360** 336
[2] Li Y J, Li S L, Gong P, Li Y L, Fang X Y, Jia Y H and Cao M S 2018 *Physica B* **539** 72
[3] Wang J, Xiong S J, Wu X L, Li T H and Chu P K 2010 *Nano Lett.* **10** 1466
[4] Hu P, Dong S, Zhang X H, Gu K X, Chen G Q and Hu Z 2017 *Sci. Rep.* **7** 3011
[5] Bekaroglu E, Topsakal M, Cahangirov S and Ciraci S 2010 *Phys. Rev. B* **81** 075433
[6] Gong P, Li Y J, Jia Y H, Li Y L, Li S L, Fang X Y and Cao M S 2018 *Phys. Lett. A* **382** 2484
[7] Li X X, Tian Y, Gao F M, Wang L, Chen S L and Yang W Y 2018 *Ceram. Int.* **44** 19021
[8] Li S Y, Li W Q, Zhao H P and Du L Z 2014 *Nanosci. Nanotech. Lett.* **6** 1091
[9] Matsunami H 2006 *Microelectron. Eng.* **83** 2
[10] Xiong S, Latour B, Ni Y, Volz S and Chalopin Y 2015 *Phys. Rev. B* **91** 224307
[11] Xin X, Yan F, Koeth T W, *et al.* 2005 *Electron. Lett.* **41** 1192
[12] Wu I J and Guo G Y 2008 *Phys. Rev. B* **78** 035447
[13] Li Y J, Li Y L, Li S L, Gong P and Fang X Y 2017 *Chin. Phys. B* **26** 047309
[14] Phan H P, Dinh T, Kozeki T, Nguyen T K, Qamar A and Namazu T 2016 *IEEE Electron Dev. Lett.* **37** 1029
[15] Zhang Z and Xu Y 2013 *Superlattice Microstructure* **57** 19
[16] Li S L, Li Y L, Li Y J, Gong P and Fang X Y 2017 *Int. J. Mod. Phys. B* **31** 1750173
[17] Ren J F, Zhang Y R, Zhang L, Yuan X B and Hu G C 2014 *Mod. Phys. Lett. B* **28** 1450195
[18] Mpourmpakis G, Froudakis G E and Lithoxoos G P 2006 *J. Samios, Nano Lett.* **6** 1581
[19] Yang L, Zhao H, Fan S M, Deng S S, Lv Q, Lin J and Li C P 2014 *Biosens. Bioelectron.* **57** 199
[20] Raynaud C 2001 *J. Non-Cryst. Solids* **280** 1
[21] Fan X, Ye R, Peng Z, Wang J, Fan A and Guo X 2016 *Nanotechnology* **27** 255604
[22] Kityk I V, Makowska-Janusik M, Kassiba A, *et al.* 2000 *Opt. Mater.* **13** 449
[23] Hua A, Wei F, Pan D S, Yang L, Feng Y, Li M Z, Wang Y, An J, Geng D Y, Liu H Y, Wang Z H, Liu W, Ma S, He J and Zhang Z D 2017 *Appl. Phys. Lett.* **111** 223105
[24] Yang H J, Cao M S, Li Y, Shi H L, Hou Z L, Fang X Y, Jin H B, Wang W Z and Yuan J 2014 *Adv. Opt. Mater.* **2** 214
[25] Zheng H, Zhang Y, Yan Y, *et al.* 2014 *Carbon* **78** 288
[26] Li H P, Fu W Y, Shen X P, Han K and Wang W H 2017 *Chin. Phys. B* **26** 127801
[27] Zhang K L, Zhang J Y, Hou Z L, Bi S and Zhao Q L 2019 *Carbon* **141** 608
[28] Zhang X, Chen Y, Xie Z, *et al.* 2010 *J. Phys. Chem. C* **114** 8251
[29] Yang Y, Yang H, Wei G D, Wang L, Shang M H, Yang Z B, Tang B and Yang W Y 2014 *J. Mater. Chem. C* **2** 4515
[30] Zhao J, Meng A, Zhang M, Ren W P and Li Z J 2015 *Phys. Chem. Chem. Phys.* **17** 28658
[31] Chen Y Q, Zhang X N and Xie Z P 2015 *ACS Nano* **9** 8054
[32] Li Y J, Li S L, Gong P, Li Y L, Cao M S and Fang X Y 2018 *Physica E* **98** 191
[33] Chen S L, Shang M H, *et al.* 2016 *J. Mater. Chem. C* **4** 7391
[34] Choueib M, Ayari A, Vincent P, Perisanu S and Purcell S T 2011 *J. Appl. Phys.* **109** 073709
[35] Li Y J, Li S L, Gong P, Li Y L, Fang X Y, Jia Y H and Cao M S 2018 *Physica E* **104** 247
[36] Li S L, Yu X X, Li Y L, Gong P, Jia Y H, Fang X Y and Cao M S 2019 *Eur. Phys. J. B* **92** 155
[37] Jia Y H, Gong P, Li S L, Ma W D, Fang X Y, Yang Y Y and Cao M S 2020 *Phys. Lett. A* **384** 126106
[38] Fang X Y, Yu X X, Zheng H M, Jin H B, Wang L and Cao M S 2015 *Phys. Lett. A* **379** 2245